Influence of air oxidation on the properties of decorative NbO$_x$N$_y$ coatings prepared by reactive gas pulsing

J.M. Chappé [a,*], P. Carvalho [a], S. Lanceros-Mendez [a], M.I. Vasilevskiy [a], F. Vaz [a], A.V. Machado [b],
M. Fenker [c], H. Kappl [c], N.M.G. Parreira [d], A. Cavaleiro [d], E. Alves [e]

[a] *Universidade do Minho, Dept. Física, Campus de Azurém, 4800-058 Guimarães, Portugal*
[b] *Universidade do Minho, Dept. Engenharia de Polímeros, Campus de Azurém, 4800-058 Guimarães, Portugal*
[c] *FEM, Dept. POT-MPh, Katharinenstr. 17, D-73525 Schwäbisch Gmünd, Germany*
[d] *ICMES - Fac. de Ciências e Tecnologia da Universidade de Coimbra, 3030-788 Coimbra, Portugal*
[e] *ITN, Departamento de Física, E.N.10, 2686-953 Sacavém, Portugal*

Available online 21 September 2007

Abstract

In this work the oxidation resistance of DC reactive sputtered niobium oxynitrides and its influence on the properties of the films are studied. The depositions have been carried out by DC magnetron sputtering with a reactive gas pulsing process. The nitrogen flow was kept constant and the oxygen flow was pulsed. Pulse durations of 10 s produced multilayer coatings with a period of $\lambda = 10$ nm. Three sets of films with increasing duty cycle (=on-time of high oxygen flow/pulse duration) have been deposited. The films were subsequently annealed in air at 400, 500 and 600 °C, respectively.

X-ray diffraction measurements showed a clear and progressive change from a roughly amorphous nature of the films to a crystalline oxide-type compound for those annealed at 600 °C, which was consistent with the composition analysis. For annealing temperatures of 500 and 600 °C, the coatings presented a significant reduction in hardness, approaching the values characteristic of Nb$_2$O$_5$-type films. Moreover, the residual stress measurements performed by using the deflection method revealed low values in all the coatings nearly independent on the annealing temperature.

Color variation in the CIE−L *a*b* color space and the reflectance in the UV–visible spectrum range of these niobium oxynitrides were investigated and correlated to their chemical composition and structural features. For both properties, the variation tendencies are quite similar, showing the transition from a nitride-type alloy to an oxide-type one with increasing annealing temperature.
© 2007 Elsevier B.V. All rights reserved.

Keywords: Niobium oxynitride; Reactive sputtering; Structure; FTIR; Hardness; Optical reflectance

1. Introduction

The number of publications per year in the field of oxynitrides increased in the last five years by a factor of 3, showing the growing importance of this relatively new class of coating material. Controlling the oxygen-to-nitrogen ratio in the oxynitride allows one to tune the film properties. The field of applications of oxynitride films is wide [1,2] but there are not many publications about NbON thin films. Beneath patents, e.g. [3], and publications from the authors [4,5], only one paper was found where NbON is applied as a CrON/NbON multilayer topcoat to increase the corrosion resistance of CrN/NbN-coated high speed steel [6].

In a former study on the Nb–O–N system [4], we reported on the pulsed power reactive magnetron sputtering of Nb, Nb–O and Nb–O–N thin films. In two further studies [1,5] we published results on the deposition of niobium oxynitride coatings using reactive magnetron sputtering in direct current (DC) and pulsed modes, where their properties such as chemical composition, morphology, crystallographic structure, electrical and optical behaviors, mechanical properties, thermal stability (in vacuum), corrosion and degradation behavior have been studied.

In order to gain better understanding of the relationships between the oxidation resistance and the structure, chemical composition, mechanical properties (hardness, residual stress),

---

and color of the coatings, the present paper reports on in-air oxidation resistance experiments of reactively gas-pulsed Nb–O–N coatings, prepared with three different pulsing conditions.

2. Experimental details

Nb–O–N coatings were deposited by DC reactive magnetron sputtering in a commercial available vacuum system (Leybold LH Z400). The base pressure was lower than 6×10^{-4} Pa. The pumping speed was 300 L s^{-1}. Prior to the depositions, the target and the substrates were sputter cleaned in pure Ar atmosphere. For the thin film deposition, a metallic niobium target (purity 99.8%) was sputtered in an Ar/O$_2$/N$_2$ atmosphere by a reactive gas pulsing process. To deposit Nb–O–N thin films with different oxygen contents, the nitrogen flow was kept constant at 2.9 sccm, whereas the oxygen flow was pulsed between a minimum and a maximum flow of 0.5 sccm and 4.2 sccm, respectively. Hence oxygen is continuously injected in the deposition chamber, even during the $(T-t_{ON})$ time (at 0.5 sccm). A mounting triangle function was used as the pulse shape for the oxygen gas flow. Pulse durations T of 10 s and duty cycles $\alpha = t_{ON}/T$ of 0.3, 0.6 and 0.9 were chosen (t_{ON} = on-time of high oxygen flow). The average target current density was kept constant at 100 A m^{-2}. Mirror polished high speed steel (AISI M2), stainless steel (AISI 316) and Si wafers with (100) orientation were used as substrates.

The depositions started at room temperature. A thermocouple located in the substrate holder showed that the temperature increased during the deposition and remained lower than 80 °C. The annealing experiments of as-deposited samples were performed in air in a furnace, at 400, 500 and 600 °C, separately and at the desired temperature during 1 h, and then removed from the furnace and left to cool down in surrounding air. The atomic compositions of the as-deposited samples and the depth concentration profiles (in the growth direction) after annealing were measured by RBS, performed with a beam energy of 1.4 MeV. The scattering angles 140° (standard detector, IBM geometry) and 180° (annular detector) were used, with tilt angles of 0° and 30°. A standard detector data was used due to the poorer resolution of the annular detector. Note that in this chamber, there is some few degree uncertainty in the incidence angle. The data were analyzed with the IBA DataFurnace NDF v8.11 [7]. For the ^{14}N and ^{16}O data, the cross sections given in [8] were used.

X-ray diffraction (XRD) experiments were performed in a Philips PW 1710 apparatus using a Cu Kα radiation ($\lambda = 0.154184$ nm) in Bragg–Brentano configuration. Infrared spectra were obtained in transmission mode on a Fourier Transform Infrared (FTIR) Perkin-Elmer 1600 spectrometer from 450 to 2000 cm^{-1}, using non-polarized light, with a resolution of 1 cm^{-1}. The hardness (H) and Young's modulus (E) of the coatings were evaluated by depth-sensing indentation technique using a Fischerscope H100, equipped with a Vickers diamond indenter, with a maximum indentation load of 30 mN. The testing procedure includes a correction of the experimental results for geometrical defects of the indenter tip, the thermal drift of the equipment and the uncertainty in the initial contact,

Table 1
Atomic composition of surface layers for as-deposited and annealed niobium oxynitride thin films

$\alpha = t_{ON}/T$	0.3		0.6		0.9	
Annealing temperature (°C)	Sum formula	Nb–O–N	Sum formula	Nb–O–N	Sum formula	Nb–O–N
As-deposited	NbO$_{0.92}$N$_{0.86}$	36–33–31	NbO$_{1.09}$N$_{0.85}$	34–37–29	NbO$_{1.28}$N$_{0.84}$	32–41–27
400	NbO$_{2.52}$N$_{0.48}$	25–63–12	NbO$_{2.52}$N$_{0.48}$	25–63–12	NbO$_{2.38}$N$_{0.46}$	26–62–12
500	NbO$_{2.52}$N$_{0.48}$	25–63–12	NbO$_{2.52}$N$_{0.48}$	25–63–12	NbO$_{2.38}$N$_{0.46}$	26–62–12
600	NbO$_{2.38}$N$_{0.46}$	26–62–12	NbO$_{2.26}$N$_{0.44}$	27–61–12	NbO$_{2.26}$N$_{0.44}$	27–61–12

as described in details elsewhere [9,10]. The residual stresses, σ_r, were calculated by the deflection method using the Stoney's equation [11], after measuring the parabolic deflections of the thin substrates (AISI 316) by laser triangulation, before and after deposition of the films [12]. The film's color was represented in the CIELAB 1976 color space by using a commercial Minolta CM-2600d portable spectrophotometer (wavelength range: 400–700 nm), with diffused illumination (D65 light source) at an 8° viewing angle (specular component excluded). Reflectance spectra of the films were obtained using a Lambda 20 UV–visible Perkin-Elmer spectrophotometer in the wavelength range 200–800 nm.

3. Results and discussion

3.1. Chemical composition, crystallographic structure and bonding states

Elemental composition measurements carried out by RBS (Table 1) on as-deposited samples show a reverse evolution of oxygen and nitrogen atomic concentrations from NbO$_{0.92}$N$_{0.86}$ for $\alpha = 0.3$ to NbO$_{1.28}$N$_{0.84}$ for $\alpha = 0.9$. These results are consistent with the increase of α and thus with the increase of the oxygen injection time within each period T. After a closer in-depth analysis, it appeared that for all films, at 400 °C, a very thin layer starts forming at the film's surface. In this surface layer, the oxygen content suddenly increased in all coatings to reach 62 and 63 at.% (O/Nb ≥ 2.38). Actually, all the surface layers exhibit a similar composition NbO$_x$N$_y$ with $2.26 < x < 2.52$ and $0.44 < y < 0.48$ (Table 1), that can be related with the formation of Nb$_2$O$_5$(N)-type compounds. The deeper part of the samples was fitted with exactly the same composition found for the as-deposited sample. At 500 °C, the oxide layer at the surface became thicker, encompassing about half the film thickness [2]. Good fits were obtained by increasing the oxygen concentration while reducing the niobium and nitrogen concentrations. The nitrogen content is rather small in this surface layer, and in fact we cannot accurately say whether there
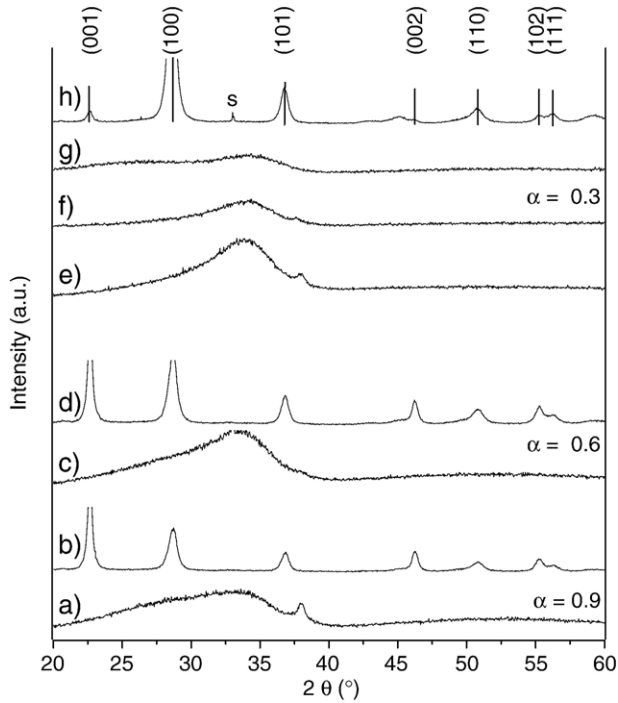
Fig. 1. X-ray diffraction patterns of niobium oxynitride thin films deposited on silicon: as-deposited (a, c and e), annealed at 400 °C (f), at 500 °C (g) and at 600 °C (b, d, h); S = substrate.

Fig. 3. Influence of the duty cycle and the annealing temperature on the hardness (full symbols) and the Young's modulus (open symbols) of niobium oxynitride films.

is nitrogen or not. At 600 °C, the oxidation process is finished and a single layer is formed with reduced niobium and increased oxygen concentration [2].

The structural evolution of the Nb–O–N coatings as a function of the annealing temperature is shown in Fig. 1. The three as-deposi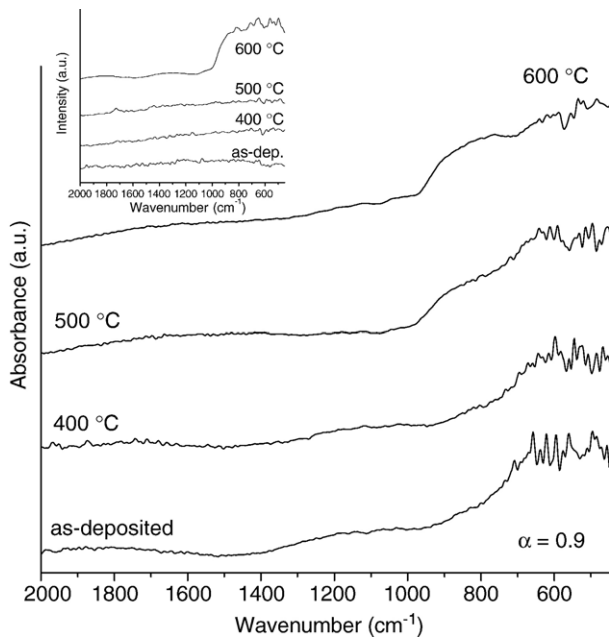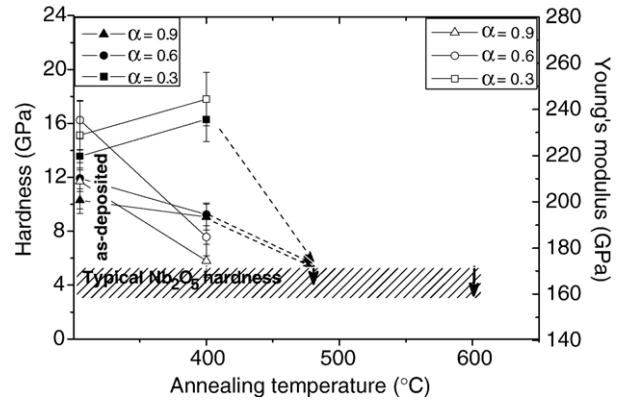ted coatings exhibit a quasi-amorphous structure (Fig. 1a, c and e). This structure is only characterized by a broad peak in the range of $2\theta = 20$–$40°$, centred at $2\theta \approx 33°$, which is not enough to identify the structure. However, there are some Nb–O–N phases that have the main diffraction peaks close to this value, see for example ICDD card 71-0177. This quasi-amorphous structure remains almost unchanged up to 500 °C, as it can be seen with the example of the coating with $\alpha = 0.3$ (Fig. 1-e, f, g and h). As already observed from the chemical compositions results, at 600 °C the coatings were totally oxidised, and then the XRD patterns exhibited by the three coatings showed a crystalline structure, identified as a hexagonal Nb_2O_5 phase, whose lattice parameters are $a = 0.3607$ nm and $c = 0.3925$ nm (ICDD card 28-0317). This hexagonal Nb_2O_5 phase was not predicted by the phase diagram of Nb–O [13], however it was usually reported in studies of niobium oxides annealed in air [14], synthetic air or in vacuum at 600 °C [1], and in argon at 500 °C [15].

Fig. 2. Infrared absorbance spectra of niobium oxynitrides thin films with $\alpha = 0.9$ and $\alpha = 0.3$ (inset).
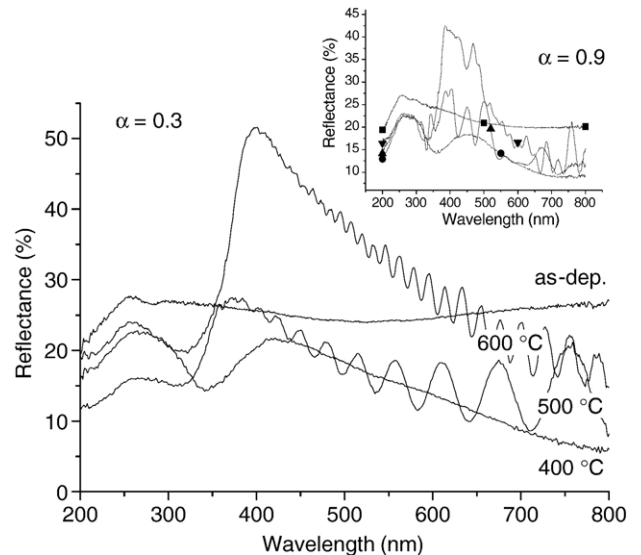

Fig. 4. Reflectance spectra of as-deposited (■), and annealed at 400 °C (●), 500 °C (▲) and 600 °C (▼) niobium oxynitride thin films on silicon substrates, deposited with $\alpha = 0.3$ and $\alpha = 0.9$ (inset).
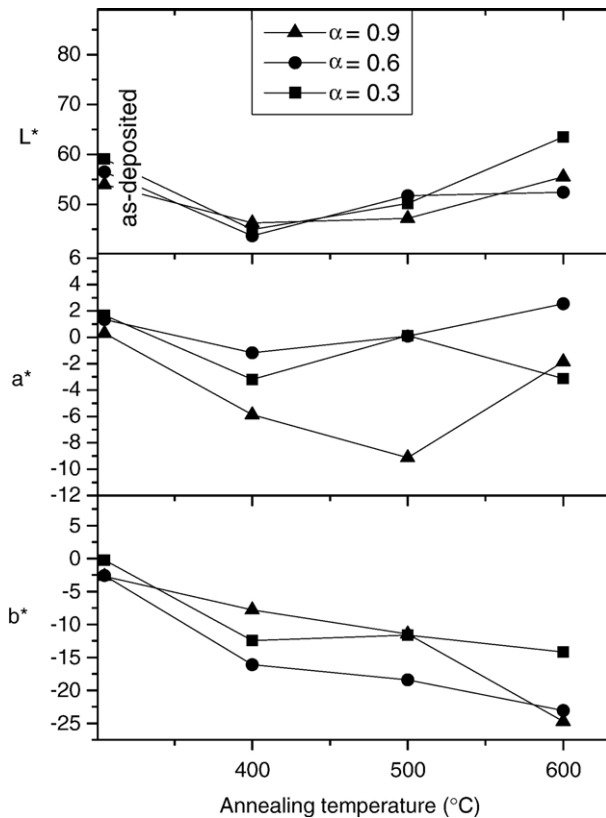
Fig. 5. Average specular colors in the CIELab 1976 color space of as-deposited and annealed niobium oxynitride thin films for various duty cycles α.

To complete this analysis, FTIR spectroscopy was used to study the evolution of the chemical structure of the films as a function of annealing temperature. The influence of the duty cycle α should also affect the film's particular arrangement and lead to changes in infrared spectra. The absorbance spectra of two coatings (calculated from the measured transmittance) are shown in Fig. 2. With increasing α, the spectra of as-deposited coatings exhibited an evolution from a typical signature of Nb–N bonds (α=0.3) [16] to the appearance of Nb–O ones seen for α=0.9. The diffuse bands in the range from 600 to 950 cm^{-1} are attributed to Nb–O stretching vibrations, as shown in literature for Nb_2O_5 compounds [17]. The spectrum corresponding to the intermediate duty cycle presented a transition regime. It means that, even if the oxygen contents in the three as-deposited films are not very different (Table 1), the presence of Nb–O bonds strongly depends on the duty cycle. After annealing at 600 °C and for all duty cycles, the spectra exhibited the same diffuse bands and a pronounced one at 800 cm^{-1}, which is typical from a Nb_2O_5 feature [18].

3.2. Mechanical properties

In order to reveal the influence of the annealing temperature on the film's properties, the mechanical properties, e.g. hardness (H) and Young's modulus (E), of the Nb–O–N coatings were analysed, as a function of the annealing temperature and for the different duty cycles (Fig. 3). At room temperature, H varies between 10.5 and 13.5 GPa, depending on the amount of oxygen present in the coatings. The coating with the lowest oxygen content exhibits the highest hardness value and the one with highest oxygen content exhibits the lowest hardness value, in agreement with the previous works from the authors [4]. After annealing at 400 °C an evolution of the hardness is observed, namely, for α=0.3, it increased from 13.5 to 16.5 GPa, and for the other two coatings, it suffers a drop to a value close to 9 GPa. Moreover, at 500 and 600 °C, the indentation occurs in the oxidised layer (the maximum indentation depth was close to 500 nm for a total thickness around 2.2 μm) since almost half or all the coating are oxidised [2]. Therefore the measured hardness value is close to the value for a homogeneous Nb_2O_5 coating, close to 6 GPa [18]. The Young modulus values of these niobium oxynitride coatings exhibited a tendency similar to that of the hardness, with $E \approx 20 \times H$. It puts in evidence the fragility and brittleness of these coatings, since this proportional law is deducted from the Griffith's theory applied to brittle materials [19]. This linear correlation between the Young modulus and the hardness was previously observed for TM–O–N coatings, like Ti–O–N [20], Zr–O–N [21] or W–O–N [10].

3.3. Optical properties

The reflectance spectra of the as-deposited coatings show little structure in the wavelength range studied (Fig. 4). This is typical of a rather strongly absorbing film on a (nearly) perfect mirror (the Si substrate, in this case). Annealing, even at the lowest temperature (400 °C), introduces some irregular large-scale oscillations in the reflectance that can be interpreted as interference fringes originating from a surface layer of few tens of nanometers in thickness. The refraction index of this nanolayer probably varies with the wavelength making the oscillations irregular. This structure is also seen in the spectra of the films annealed at higher temperatures. At the same time, the changes in the film's bulk, due to the oxidation process, occur at 500 °C and 600 °C, which produce the regular smaller scale oscillations in the reflectance spectra (Fig. 4). These changes imply an increasing transparency of (some part of) the film, propagating from the surface towards the substrate and probably associated with the oxidation of the coating. The interference fringes allow us to determine the optical thickness of the transparent region beneath the surface layer, according to the formula

$$d_{TR}^* = \frac{\lambda_m}{2} \frac{1 + (\Delta\lambda'/\Delta\lambda)}{1 - (\Delta\lambda'/\Delta\lambda)},$$

where λ_m corresponds to a maximum of the reflectance and $\Delta\lambda$ and $\Delta\lambda'$ are the distances from it to the adjacent maxima to the right and to the left, respectively. This gives, for the films grown with α=0.3, d_{TR}^*=2.17 μm (annealed at 500 °C) and d_{TR}^*=6.65 μm (600 °C). Taking the refraction index as for pure Nb_2O_5, $\eta \approx 2.3$ [15], we obtain for the real thickness of the transparent region, $d_{TR}=d_{TR}^*/\eta$, the values of 0.94 μm (500 °C) and 2.89 μm (600 °C). Comparing the latter result to the overall thickness of the deposited coating (d_0=2.2–2.3 μm), we conclude that annealing at 600 °C makes the whole film

transparent, so that the multiple reflections responsible for the small scale interference fringes occur at the coating/substrate interface. The 25–30% disagreement between d_{TR} and d_0 can be attributed to a higher value of the refraction index of the transparent region (compared to that of pure Nb_2O_5), which is possible because of the presence of a significant amount of nitrogen in the coating.

The three films start exhibiting some blue dots after 400 °C thermal treatment, which is characteristic of an interferential color resulting from the oxidation of 5% of the coating, giving a transparent top layer. For higher temperatures, the apparent color of the annealed films is milky-blue (in agreement with the measured reflectance spectra), in contrast to the uncharacteristic dark green-brownish color of the as-grown coatings. The growth parameter α has a significant influence on the average specular colors of the films (Fig. 5). We would like to emphasize that the apparent color of the coating is determined mostly by the nanometric surface layer producing the reflection peak in the 350–500 nm range for the films annealed at higher temperatures (Fig. 4). The multiple reflections at the coating/substrate interface produce only a second-order effect resulting in the interference-like tones of the coatings. The increased lightness (L^*) of the films annealed at 600 °C is correlated with their higher transparency discussed above.

4. Conclusion

The reactive gas pulsing process was successfully used to deposit niobium oxynitride thin films by DC reactive sputtering. The influence of the shape of the pulsing pattern of oxygen on the atomic composition was investigated by RBS, ranging from $NbO_{0.92}N_{0.86}$ to $NbO_{1.28}N_{0.84}$. Then the coatings were submitted to annealing in order to study the thermal stability of structural, mechanical and optical properties. The oxidation process inside the coating was also quantified by RBS.

The FTIR analysis revealed the presence of Nb–O bonds in the as-deposited film with the highest content of oxygen and in all the coatings annealed at 600 °C. Structural characterization showed that the films annealed at 600 °C exhibited peaks corresponding to Nb_2O_5 phase, whatever the original oxygen content was, while they remained amorphous for lower temperatures. Hardness measurements revealed a significant stability of the coatings at 400 °C and a slight increase for the lowest oxygen content. For higher temperatures, the hardness decreased to reach values peculiar to niobium pentoxide. A typical colorimetric study proved that the niobium oxynitride films become blue with interference-like tones. The reflectance analysis confirmed the crystallization of the films after annealing at 600 °C.

References

[1] M. Fenker, P. Carvalho, H. Kappl, F. Vaz, unpublished results.
[2] E. Alves, N. Barradas, J.M. Chappé, S. Lanceros-Méndez, F. Vaz, M. Fenker, H. Kappl, unpublished results.
[3] V. Gorokhovsky, N. Bekesch, US Patent US2002102400 (2002).
[4] M. Fenker, H. Kappl, K. Petrikowski, R. Bretzler, Surf. Coat. Technol. 200 (2005) 1356.
[5] M. Fenker, H. Kappl, O. Banakh, N. Martin, J.F. Pierson, Surf. Coat. Technol. 201 (2006) 4152.
[6] T. Savisalo, D.B. Lewis, P.Eh. Hovsepian, Surf. Coat. Technol. 200 (2006) 2731.
[7] N.P. Barradas, C. Jeynes, R.P. Webb, Appl. Phys. Lett. 71 (1997) 291.
[8] A.R. Ramos, A. Paúl, L. Rijniers, M.F. da Silva, J.C. Soares, Nucl. Instrum. Methods Phys. Res., B Beam Interact. Mater. Atoms 190 (2002) 95.
[9] J.M. Antunes, A. Cavaleiro, L.F. Menezes, M.I. Simões, J.V. Fernandes, Surf. Coat. Technol. 149 (2002) 27.
[10] N.M.G. Parreira, N.J.M. Carvalho, F. Vaz, A. Cavaleiro, Surf. Coat. Technol. 200 (2006) 6511.
[11] G.G. Stoney, Proc. R. Soc. Lond. [A] 82 (1909) 172.
[12] F. Vaz, L. Rebouta, Ph. Goudeau, J.P. Rivière, E. Schäffer, G. Kleer, M. Bodmann, Thin Solid Films 402 (2002) 195.
[13] T.B. Massalski, H. Okamoto, P.R. Subramanian, L. Kacprzak, Binary Alloy Phase Diagrams, ASM International, 1990.
[14] F. Lai, M. Li, H. Wang, H. Hu, X. Wang, J.G. Hou, Y. Song, Y. Jiang, Thin Solid Films 488 (2005) 314.
[15] S. Venkataraj, R. Drese, Ch. Liesch, O. Kappertz, R. Jayavel, M. Wuttig, J. Appl. Phys. 91 (8) (2002) 4863.
[16] M. Benkahoul, C.S. Sandu, N. Tabet, M. Parlinska-Wojtan, A. Karimi, F. Lévy, Surf. Coat. Technol. 188–189 (2004) 435.
[17] J.-P. Masse, H. Szymanowski, O. Zabeida, A. Amassian, J.E. Klemberg-Sapieha, L. Martinu, Thin Solid Films 515 (2006) 1674.
[18] S. Venkataraj, R. Drese, O. Kappertz, R. Jayavel, M. Wuttig, Phys. Status Solidi, A Appl. Res. 188 (3) (2001) 1047.
[19] S. Veprek, A.S. Argon, J. Vac. Sci. Technol., B 20 (2) (2002) 650.
[20] J.-M. Chappé, N. Martin, J. Lintymer, F. Sthal, G. Terwagne, J. Takadoum, Appl. Surf. Sci. 253 (2007) 5312.
[21] P. Carvalho, F. Vaz, L. Rebouta, L. Cunha, C.J. Tavares, C. Moura, E. Alves, A. Cavaleiro, P. Goudeau, E. Le Bourhis, J.P. Rivière, J.F. Pierson, O. Banakh, J. Appl. Phys. 98 (2005) 023715.